Visualization and Flowfield Measurements of the Vortical Flow over a Double-Delta Wing

Myong-Hwan Sohn* and Young-IL Jang**
Department of Aerospace Engineering
Korea Air Force Academy, ChungBook-Do, Korea 363-849

Abstract

The vortical flow of a 65-deg flat plate delta wing with a leading edge extension(LEX) was examined through off-surface visualization, 5-hole probe and hot-film measurements. The off-surface flow visualization technique used micro water droplets generated by a home-style ultrasonic humidifier and a laser beam sheet. The angles of attack ranged from 10 to 30 degrees, and the sideslip angles ranged from 0 to -15 degrees. The Reynolds number was 1.82×10^5 for the flow visualization, and 1.76×10^6 for the 5-hole probe and hot-film measurements. The comparison of the visualization photos and the flow field measurement showed that the two results were in a good agreement for the relative position and the structure of the wing and LEX vortices, even though the flow Reynolds numbers of the two results were much different. The wing vortex and the LEX vortex coil each other while maintaining a comparable strength and identity at zero sideslip. Neither a looping of the wing vortex around the strake vortex, nor the lopsided coiling of the stronger strake and the weaker wing vortices was observed. At non-zero sideslip, the downward movement of the LEX vortex when going downstream was enhanced on the windward side, and the downward and inboard movement of the LEX vortex when going downstream was suppressed on the leeward side. The counterclockwise coiling of the wing and LEX vortices was decreased significantly on the leeward side.

Key Word : off-surface visualization, 5-hole probe, wing vortex, LEX vortex, sideslip, coiling of vortices

Introduction

The delta wing having strake, or leading edge extension(LEX), is known to improve the aerodynamic performance of a delta wing, especially at high angles of attack. The improved aerodynamic performance is brought by the interaction of the vortices generated from the strake and the main wing, which energizes and stabilizes the vortex system, and so delays the breakdown of them. As a result, the nonlinear vortex lift is increased compared to that of the delta wing-alone configuration. However, the situation is more complicated and not always in better-aerodynamic-performance, when the sideslip angle exists. At sideslip the effective sweep angles of the two sides of the wing(windward and leeward) and the interaction state of the strake and wing vortices of the windward and leeward sides are different. On the windward side, the strake and wing vortices break down at much lower angles of attack. On the leeward side, the strake and wing vortices migrate outboard and upward from the wing surface, and their interaction is suppressed. The suction pressure distribution on the wing upper surface,

* Professor
E-mail : myongsohn@hanmail.net, TEL : 043-290-6050, FAX : 043-298-6160
** Instructor

which is the main source of the nonlinear vortex lift, changes dramatically both in the chordwise and spanwise directions. This change of the suction pressure distribution causes the pitching and rolling moment instability of the delta wing configuration at sideslip. Therefore, the complicated vortical flow of a delta wing with the strake in sideslip requires more research in order to fully exploit the vortex lift.

There have been a number of studies on the vortical flow of a delta wing with strake or LEX. References 1-7 are some of the recent studies. The experimental methods employed in these studies include force and moment balance measurement, on and off-surface flow visualization, wing surface pressure measurement and the flow field measurement. Each method has its own advantages and limitations. Therefore, a couple of complementing methods were simultaneously used in each study. This study examines the vortical flow of a delta wing with LEX in a sideslip through off-surface visualization, 5-hole probe and hot-film measurements of the wing leeward flow region. The off-surface flow visualization technique used micro water droplets and a laser beam sheet. The angles of attack ranged from 10 to 30 degrees, and the sideslip angles ranged from 0 to -15 degrees. The analysis was focused on how the structure, interaction and breakdown of vortices depend on angle of attack and sideslip angle.

Experimental Model, Facility and Technique

Experimental Model

Figure 1 shows the geometry and a photograph of the delta wing/LEX model used in the 5-hole probe and hot-film measurements of the wing leeward flow region. The model is a flat wing with a 65° sweep angle and a sharp leading edge. The sharp leading edge was obtained by beveling 25° on the lower surface, leaving the upper surface flat. The trailing edge was also beveled in the same way. The model has the root chord of 795 mm including the LEX, and the trailing edge has a span of 475.4 mm. The thickness of the wing section is 15 mm. The LEX is also a 6.35 mm thick flat plate, and has symmetrically beveled leading and side edges. The platform of the LEX has the sweep angles of 65° and 90°.

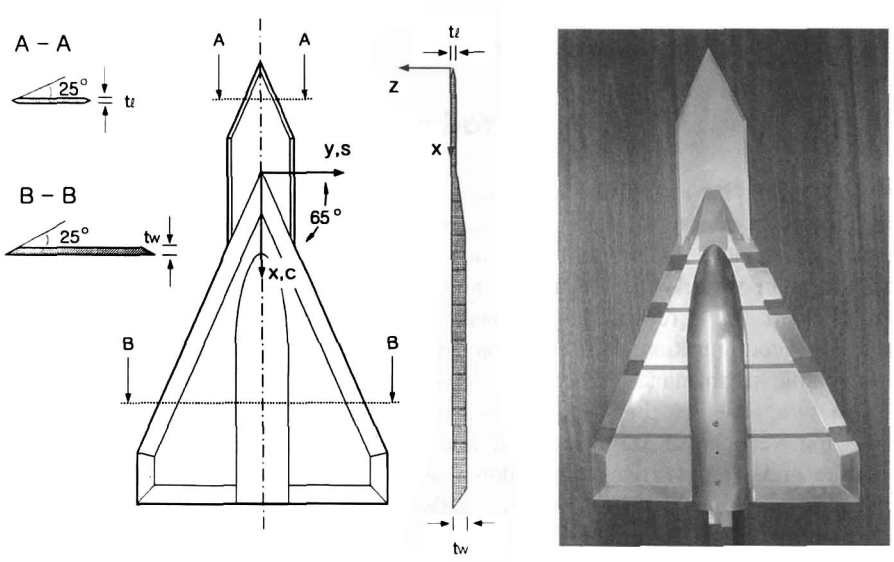

(a) Geometry of model

(b) Photograph of the model (lower surface)

Fig. 1. Geometry and photograph of the experimental model

Off-surface Visualization of the Wing Leeward Flow Region

The off-surface flow visualization was made with a 2/3 reduced model, which had the same planform geometry as that of the model used in the 5-hole probe and hot-film measurements. An off-surface flow visualization method of using micro water droplets and a laser beam sheet was developed for this study. Water droplets of size 5~10 μm was generated from a home-style ultrasonic humidifier. To simulate the fluid flow exactly in the visualization, the micro water droplets had to meet a couple of requirements: a small diffusion rate and a small sedimentation velocity. The two requirements are somewhat contradictory because the sedimentation velocity increases with the droplet size, whereas the diffusion rate decreases with it. Assuming the water droplet is a spherical particle, sedimentation velocity can be expected. By applying Stokes law, the sedimentation velocity of a particle, V_s, is given by

$$V_S = \frac{g d_P^2}{18 \nu_F} (\rho_P / \rho_F - 1) \tag{1}$$

where d_p is the diameter of a spherical particle, ρ_p is the density of a particle, ρ_F is the fluid density, ν_F is the kinematic viscosity of the fluid, and g is the gravitational acceleration.

The marking particles will follow the flow exactly if the sedimentation velocity V_s is zero. However, since the condition ρ_p / ρ_F =1 can not always be satisfied, the marking particles should be as small as possible. If one requires the particle to sediment during the time period of an experimental observation, $\triangle t_{exp}$, by not more than one particle diameter, the appropriate size of the particle is determined by

$$d_P \leq \frac{18 \nu_F}{g \Delta t_{exp} (\rho_P / \rho_F - 1)} \tag{2}$$

From equation (2), the diameter of the water droplet has to be less than 1.5 μm by using the standard values of the water droplet and air densities, the air viscosity, and the free stream velocity(6.2 m/sec) as the passing time of the marking particle. Thus, the size of micro water droplets used in the present study, 5~10 μm, is still large. However, since the sedimentation of the micro water droplet is about 0.2~0.3 mm at the middle region of the wing, and 0.5~0.6 mm at the trailing edge region, the size of water droplets used is considered to be acceptable for the flow visualization. The diffusion rate is influenced by the droplet size and environmental conditions. It requires temperature control in order to reduce the diffusion rate of the water droplet. However, the diffusion rate is not significant in the present experimental study since the passing time of the water droplet in the target flow region is significantly smaller than the diffusion time.

A 3 W Argon ion laser was used to generate a light sheet. The laser light sheet was made by a cylindrical lens, and a convex focusing lens was used to interrogate specific cross

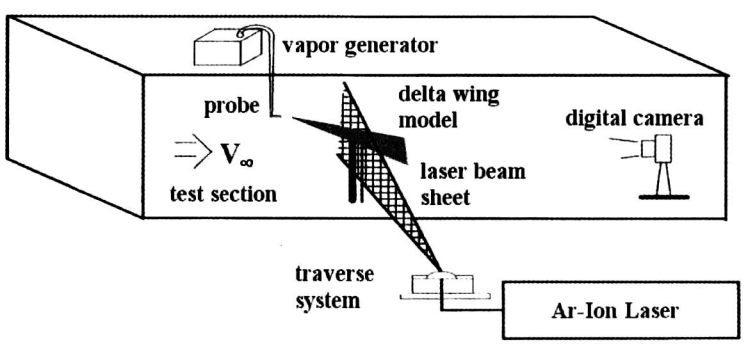

Fig. 2. Schematic diagram of the visualization experimental set-up

sections of the vortical leeward flow region. The laser light sheet was perpendicular to the wing surface. The illuminated planes were recorded by a high-resolution digital camera. The off-surface flow visualization was performed in a low-speed wind tunnel with a test section size of 0.9 m(W)×0.9 m(H)×2.1 m(L). The free stream velocity of the flow visualization was 6.2 m/s, which corresponds to the Reynolds number of 1.82×10^5. Figure 2 shows the experimental set-up of the off-surface flow visualization technique using the micro water droplet and the laser beam sheet employed in the present study.

5-Hole Probe Measurements of the Wing Leeward Flow Region

The 5-hole probe was employed to measure the total pressure and cross flow velocity vectors of the cross-section of the wing leeward flow region. The 5-hole probe used has a spherical nose of diameter 3.175 mm, and length 30.48 mm. The 5-hole probe was calibrated by employing the non-nulling method. The calibration result showed that the 5-hole probe measures the velocity vector angle with an accuracy of less than 3% for a pitch angle below 45°. The data of 5-hole probe measurement was an ensemble average taking 300 signals. The details of the 5-hole probe measurement are described in reference 4. The total pressure field of the wing leeward flow region is represented by a color-coded coefficient contour. The total pressure coefficient is defined as $Cp_t=(P_t - P_{t\infty})/q_\infty$, where P_t is the total pressure of a point, $P_{t\infty}$ is the total pressure of the free stream and q_∞ is the dynamic pressure of the free stream. Therefore, the total pressure coefficient in the present study can be considered as the total pressure loss coefficient. The 5-hole probe measurement of the wing leeward flow region was done in another low-speed wind tunnel that has a test section of 3.5 m(W)×2.45 m(H)×8.7 m(L). The free stream velocity was 40 m/s, which corresponds to the Reynolds number of 1.76×10^6.

Results and Discussions

In the present study, x is the coordinate along the wing centerline, measured from the wing apex, y is the coordinate along the wing span measured from the wing centerline, and z is the height above the upper wing surface.

Comparison of Visualization and 5-hole Probe Measurements

Figure 3 compares the visualization section photos of the wing leeward flow region and the cross flow velocity and total pressure coefficient distribution of the wing leeward flow region by 5-hole probe measurement at the 43% chord station, where two distinct pairs of wing and LEX vortices are observed. The comparison shows that the two results have a remarkable agreement in relative positions and the structures of the wing and LEX vortices, even though the flow Reynolds numbers of the two results are much different (1.82×10^5 for visualization, 1.76×10^6 for 5-hole probe measurement).

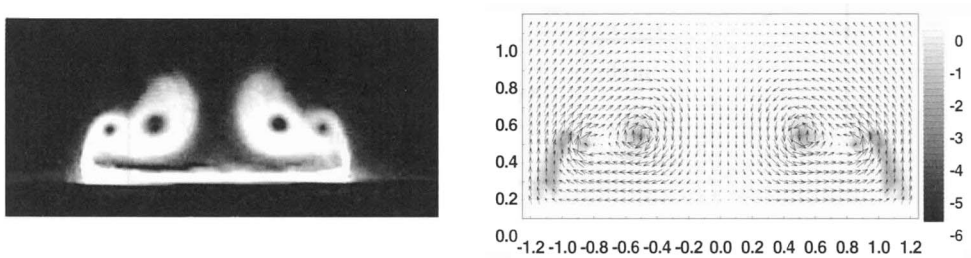

(a) Section photo (b) Cross flow velocity and total pressure contour

Fig. 3. Comparison of section photo by visualization and cross flow velocity and total pressure contour by 5-hole probe (α=24°, β=0°, x/c=0.43)

For example, the shear layer connecting the wing leading edge and the wing vortex core is observed both in the visualization photo and the total pressure contour. The size of the LEX vortex is larger than that of the wing vortex. Table 1 compares the vortex core positions of the visualization result and the 5-hole probe measurement. The vortex core position in the visualized photo is assumed to be the center of the black dot, and the 5-hole probe assumed the position of the maximum absolute value of the total pressure coefficient. In Table 1, s denotes the local semi-span of the model wing. Table 1 shows that the two results have a good agreement of the vortex core positions within the observation error.

Table 1. Comparison of vortex core locations from visualization and 5-hole probe measurement (α=24°, β=0°, x/c=0.43, starboard wing)

	Wing vortex	LEX vortex
Visualization	y/s=0.80 z/s=0.35	y/s=0.47 z/s=0.38
5-hole probe	y/s=0.80 z/s=0.40	y/s=0.52 z/s=0.42

Comparison of 5-hole Probe and Hot-film Measurements

Figure 4 compares the total pressure coefficient distribution of the wake section obtained by 5-hole probe measurement and the velocity field by the hot-film anemometer at the 43% chord station. Figs. 4(a) and (b) are for zero sideslip, whereas Figs. 4(c) and (d) are for -5° sideslip angle. In Fig. 4(a) which is the total pressure coefficient distribution by 5-hole probe, the LEX vortex separated in the mid-span region and the wing vortex connected to wing

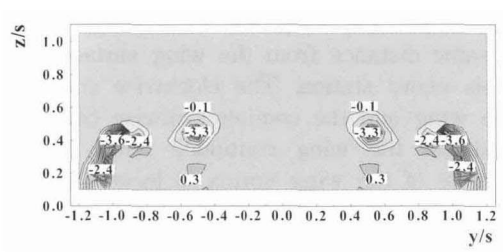

(a) Total pressure field by 5-hole probe (α=24°, β=0°, x/c=0.43)

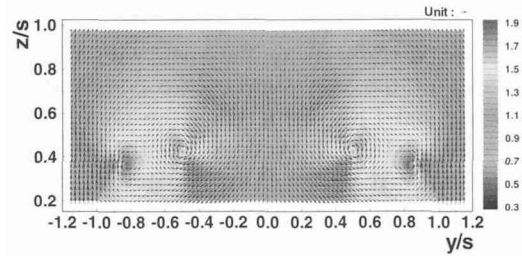

(b) Velocity field by hot-film (α=24°, β=0°, x/c=0.43)

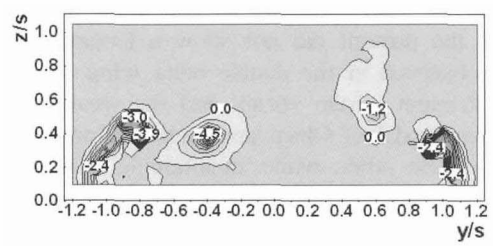

(c) Total pressure field by 5-hole probe (α=24°, β=-5°, x/c=0.43)

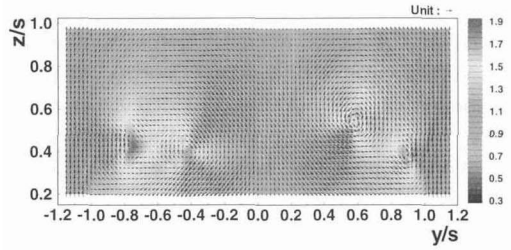

(d) Velocity field by hot-film (α=24°, β=-5°, x/c=0.43)

Fig. 4. Comparison of total pressure field by 5-hole probe and velocity field by hot-film anemometer

leading edge are shown. The minimum value of the total pressure coefficient for the LEX vortex was -3.6 at y/s=0.52 and z/s=0.42, while that for the wing vortex was -2.4 at y/s=0.85 and z/s=0.40. Assuming a location at which the value of the total pressure coefficient is minimum as the vortex core, it was observed that the vortex core predicted by the 5-hole probe measurement is located slightly outboard and upward from the wing surface compared to the visualization result. Figure 4(b) is the cross flow velocity vectors and the axial velocity contour obtained by the 3-axis hot-film anemometer at the same flow condition of the 5-hole probe measurement. Assuming a location at which the axial velocity is maximum as the vortex core, the u/U value of the LEX vortex core was 1.6 at y/s=0.55 and z/s=0.475, while that of the wing vortex was 1.9 at y/s=0.825 and z/s=0.375. Figures 4(c) and (d) show that the LEX and wing vortices of the windward side are stronger than those of the leeward side at $\beta=-5^{\circ}$. In Fig. 4(c), the minimum value of the total pressure coefficient for the LEX and wing vortices of the windward side was -4.5 and -3.9, respectively, while that for the LEX and wing vortices of the leeward side was -1.2 and -2.4, respectively. The 5-hole probe result(Fig.4(c)) shows that the LEX vortex is stronger than the wing vortex on the windward side. The hot-film result(Fig.4(d)) shows that the wing vortex is stronger than the LEX vortex on the windward side. This disagreement in the prediction of vortex strengths at non-zero sideslip condition is discouraging. However, both the 5-hole probe and the hot-film measurements show a good agreement in the relative position and structure of the wing and LEX vortices.

Vortex Structure, Interaction and Breakdown

Figure 5 shows the chordwise development and the interaction of the wing and LEX vortex pairs at the 24 degrees of angle of attack and the zero sideslip angle. At 30% chord station(Fig.5 (a)), the wing leeward flow region is dominated by a symmetric LEX vortex pair of circular shapes, and the wing vortex starts to develop at the wing leading edge. At further downstream the wing vortex grew and migrated upward, and the LEX vortex migrated downward and inboard. At 45.6% chord station(Fig. 5 (e)), the wing and LEX vortices were positioned laterally along the span with the nearly same distance from the wing surface. Also the sizes of the two vortices are comparable at this chord station. The clockwise coiling of the wing and LEX vortices on the port side of the wing and the counterclockwise coiling of the wing and LEX vortices on the starboard side of the wing continued when flowing downstream. At 60.5% chord station(Fig. 5(h)), the core of the wing vortex is located directly above the core of the LEX vortex. So, the wing vortex and the LEX vortex each rotate 90 degrees from the 45.6% chord station(Fig. 5(e)) to the 60.5% chord station(Fig. 5(h)). The wing and LEX vortices continued coiling without merging up to the 75.4% chord station(Fig. 5(k)), after which the two vortices start to merge. The excellent symmetry of the vortex system on the port and the starboard sides of the wing was maintained up to the last chord station without any vortex breakdown. The interaction and structure of the wing and LEX vortices of the delta wing/LEX model examined in the present did not show a looping of the wing vortex around the strake vortex, which was observed in the double delta wing model of Hoeijmaker et al.[5], nor the lopsided coiling of the stronger strake vortex and the weaker wing vortex, which was observed in the double delta wing model of Olsen and Nelson[1]. Instead, the wing vortex and the LEX vortex in Fig. 5 coil each other while maintaining comparable strength and identity. The last slice in Fig. 5 shows that the wing and LEX vortices merge into a single vortex without breakdown at the trailing edge position(x/c=1.0). The vortex characteristics are closely related to the suction pressure on the wing upper surface. The high suction pressure on the upper surface of delta wings at high angles of attack is due to the strong vortices in the wing leeward flow region. The relation between the suction pressure distribution and the vortex flow characteristics of the delta wing with LEX is presented in references 4 and 10.

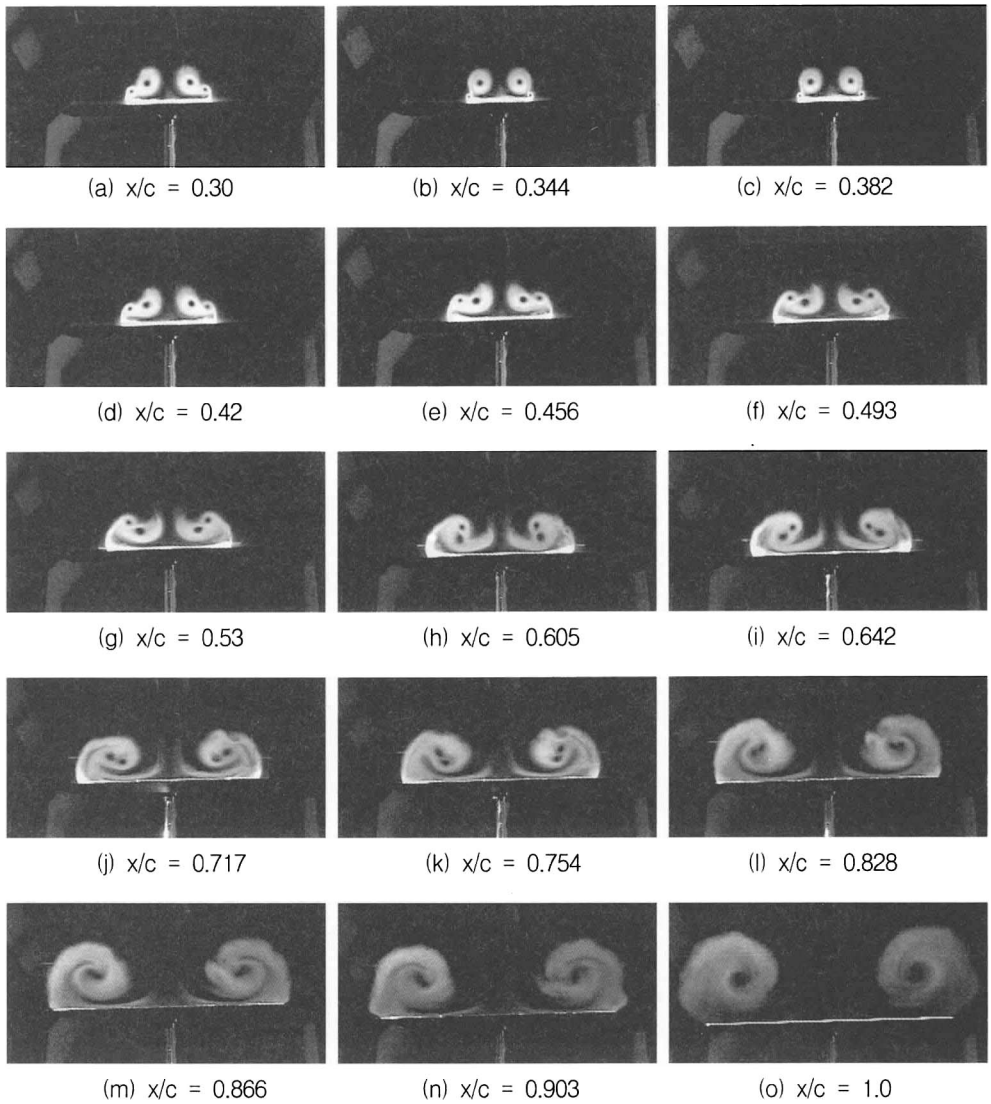

Fig. 5. Vortex development and interaction along the chordwise direction (α=24°, β=0°)

Figure 6 shows the chordwise development and the interaction of the wing and LEX vortex pairs at α=24° and β=-5°. It is observed that the sideslip angle of -5° destroys the symmetry of the vortex system on the two sides of the wing, and changes the interaction state of the wing and LEX vortices on the two sides of the wing dramatically. The downward movement of the LEX vortex as going downstream is enhanced on the windward side, and the downward and inboard movement of the LEX vortex as going downstream is suppressed on the leeward side. Also the counterclockwise coiling of the wing and LEX vortices is delayed significantly on the leeward side. The wing and LEX vortices of the windward side break down before reaching the last chord station. The major effect of the sideslip angle was to expedite the vortex breakdown on the windward side and to delay it on the leeward side. The expedited vortex breakdown on the windward side and the delayed vortex breakdown on the leeward side observed in Fig. 6 was also observed in the study of Hebbar et al.[3] where a flow visualization of the vortical flow over a straked delta wing of 76/40 degree sweep angles was made in the water tunnel.

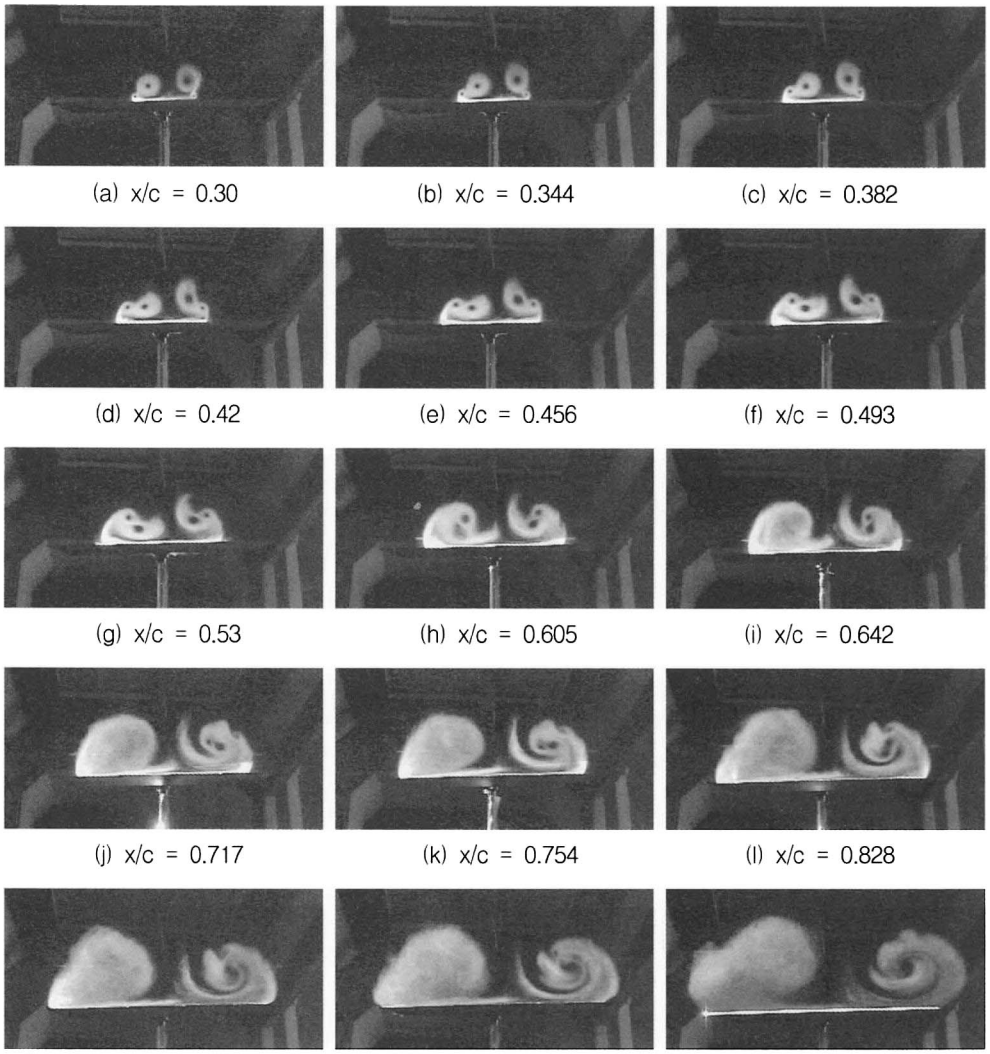

Fig. 6. Vortex development and interaction along the chordwise direction (α=24°, β=−5°)

Figure 7 illustrates the trajectory of the core position of the wing and LEX vortices in the y-z plane as a function of the angle of attack and the sideslip angle. The core positions were obtained from the dynamic images of visualization. The line of sight of the camera was in parallel to the wing surface to avoid any distortion in the z-direction. In Fig. 7, the windward wing vortex core starts its trajectory in the vicinity of the leading edge of the port wing(-y axis), and spirals clockwise as going downstream. The leeward wing vortex core starts its trajectory in the vicinity of the leading edge of the starboard wing(+y axis), and spirals counterclockwise as going downstream. The starting position was at the 30% chord position.

The LEX vortex core starts its trajectory from the mid-span of the wing leeward region. Figures 7(a) and (b) show that the increase of the angle of attack from 12° to 24° shifts the core positions of the wing and LEX vortices farther inboard and upward than the zero sideslip case. This tendency is the same as in other studies [1, 8] of the double delta wings. At high angle of attack, the wing vortex core makes a stronger spiraling when going downstream, and the coiling of the wing and LEX vortices is enhanced. At the sideslip angle of -10°(Figs. 7(c)

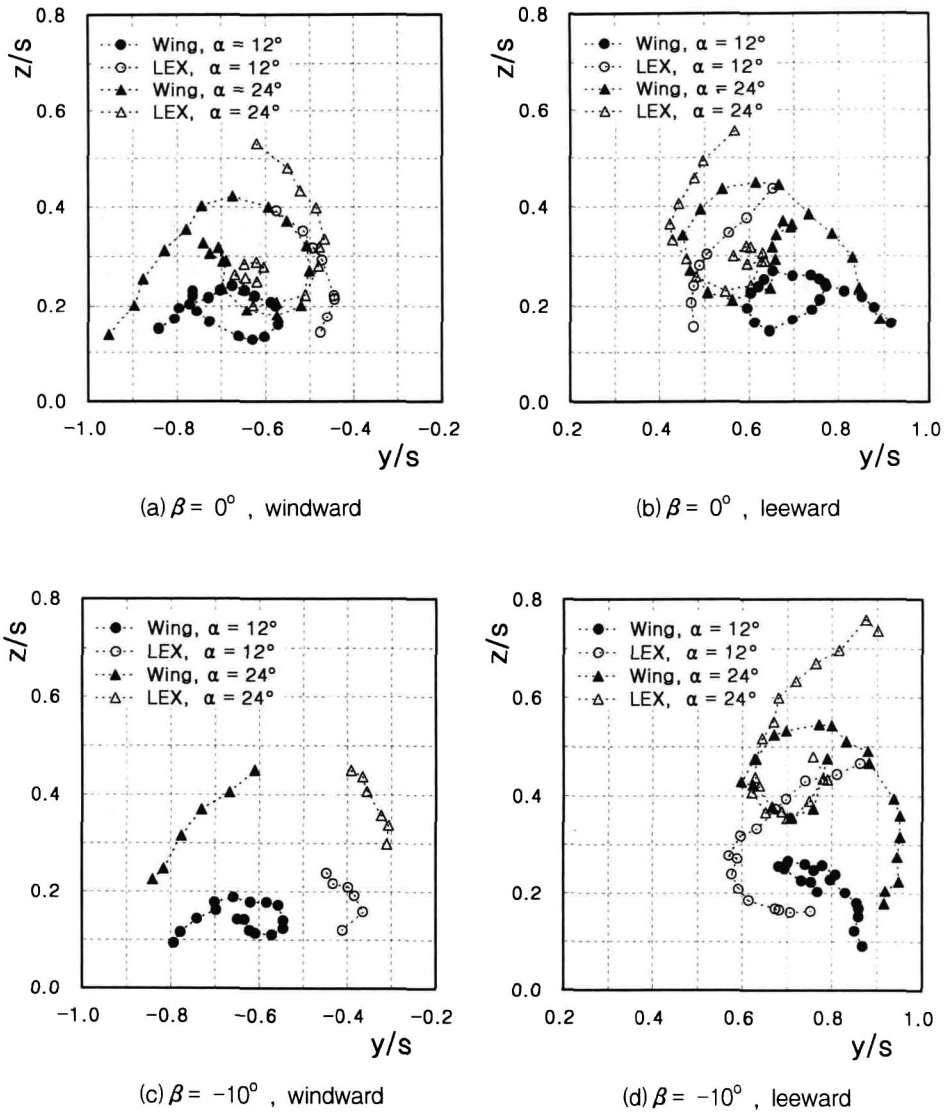

Fig. 7. Vortex core trajectory in the y-z plane depending on angle-of-attack

and (d)), the increase of the angle of attack from 12° to 24° shifts the wing and the LEX vortex cores almost vertically, especially on the leeward side. The amount of vertical shift is much greater than the zero sideslip angle case. At β=-10°, the windward wing vortex breaks down before reaching the last chord station as shown in Fig. 7(c).

Figure 8 isolates the effect of sideslip on the vortex core trajectory at a fixed 20° angle of attack. At the zero sideslip angle, the position of the port wing vortex core was about y/s= -0.91 and z/s=0.15, and the position of the port LEX vortex core was about y/s= -0.6 and z/s=0.51 at the 30% chord station. The port wing vortex migrated inboard and upward, and the port LEX vortex migrated inboard and downward up to a certain chord station, after which they migrated downward(wing vortex) or upward(LEX vortex). The clockwise-rotating wing and LEX vortices coil each other as going downstream. The center of the port wing vortex core was between y/s= 0.91(at the 30% chord station) and y/s= 0.5(at the 68% chord

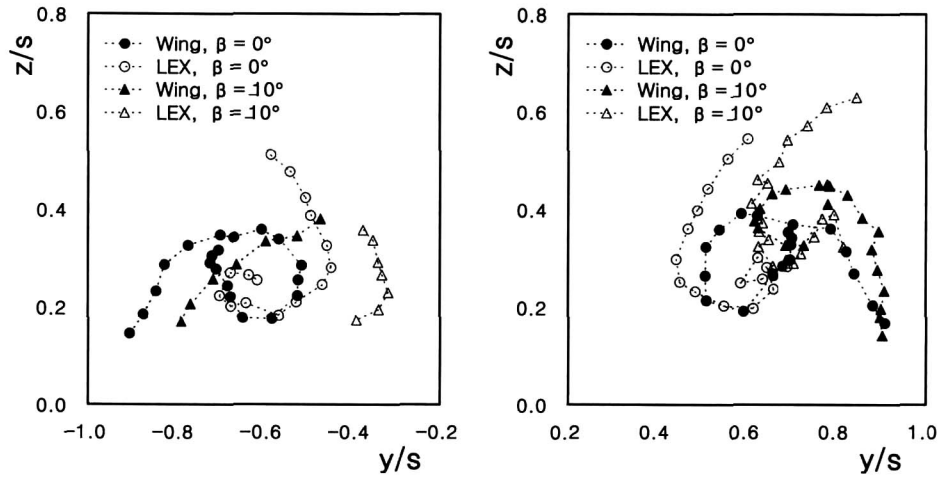

(a) windward (b) leeward

Fig. 8. Vortex core trajectory in the y-z plane depending on sideslip angle(α=20°)

station). The center of the port LEX vortex core was between y/s= 0.7 (at the 72% chord station) and y/s= 0.4(at the 48% chord station). The sideslip angle shifts the wing and the LEX vortices inboard, and expedites the breakdown of them on the windward side. On the leeward side, the sideslip angle shifts the wing and the LEX vortices outboard and upward. Also the wing and LEX vortices coil each other without breakdown up to the last chord station.

The effect of angle of attack and sideslip angle on the behavior of the vortical flow can be seen more clearly in the total pressure coefficient maps on the transverse plane. Figure 9 shows the total pressure coefficient distribution at the 30% chord station section for two different angles of attack, 16° and 28°. The sideslip angle is zero. It is observed that the total pressure maps of the two different angles of attack are similar in structure, but significantly different in magnitude. At the higher angle of attack, the wing leeward flow region is dominated by the strong LEX vortex pair, which was fed with vorticity generated in the boundary layer in the vicinity of the sharp leading edge.

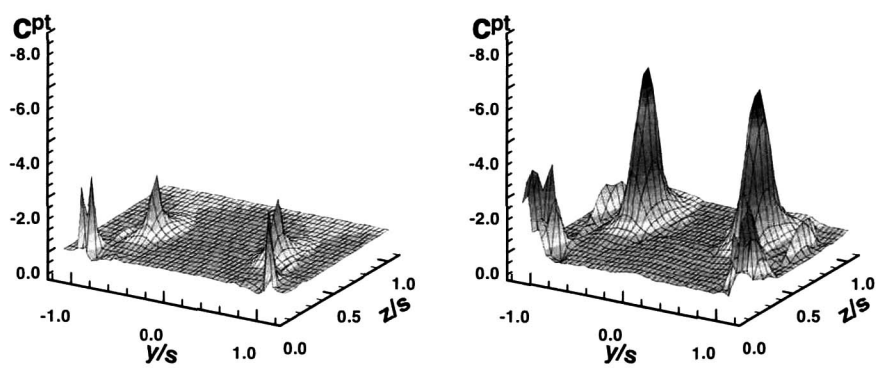

(a) α=16° (b) α=28°

Fig. 9. Total pressure coefficient distribution depending on angle of attack (β=0°, x/c=0.30)

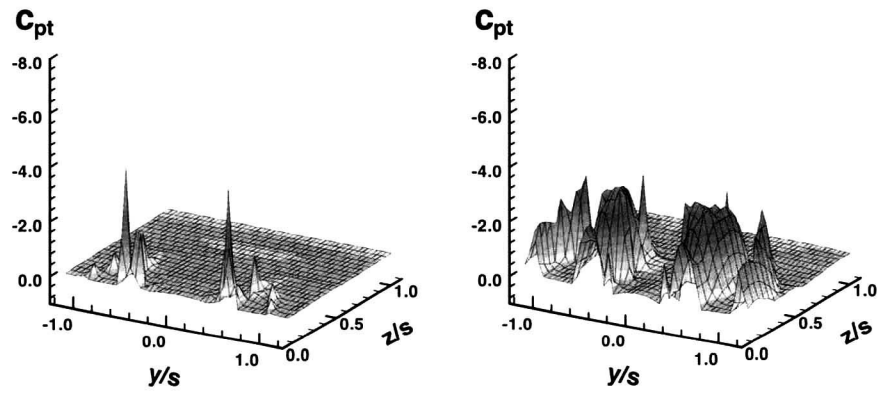

(a) α=16° (b) α=28°

Fig. 10. Total pressure coefficient distribution depending on angle of attack (β=0°, x/c=0.60)

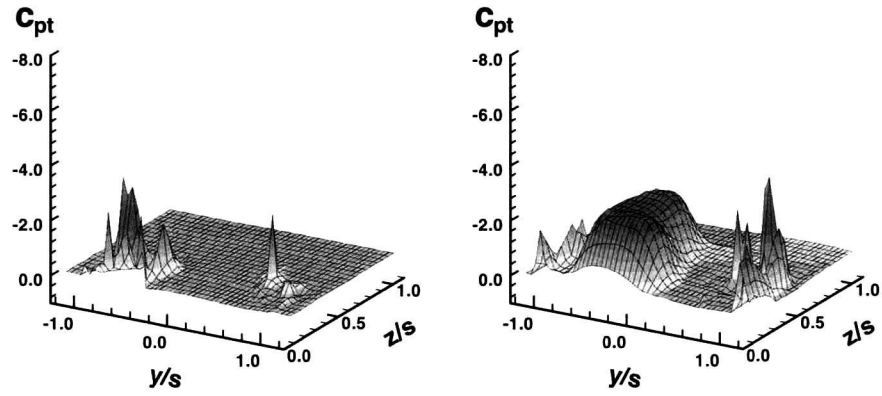

(a) α=20° (b) α=28°

Fig. 11. Total pressure coefficient distribution depending on angle of attack (β=−10°, x/c=0.60)

Figure 10 compares the total pressure coefficient distributions of the two different angles of attack, 16° and 28°, at 60% chord station section. The sideslip angle is zero. Figure 10 shows that, at the 60% chord station, the total pressure maps of different angles of attack are much different both in structure and magnitude. At the lower angle of attack, the wing and LEX vortices are moved to a mid-span region of each side of the wing in a highly concentrated state. The wing and LEX vortices are close to each other, but do not merge. At the higher angle of attack, the total pressure coefficient distribution corresponding to the LEX vortex indicates the beginning of vortex breakdown, which is characterized by the collapse of a spiked C_{pt} distribution as shown in Fig. 10(b).

Figure 11 compares the total pressure coefficient distributions of α=20° and α=28° at the 60% chord section, for sideslip angle −10°. By sideslip, the symmetry of the vortex pairs on the two sides of the wing is destroyed, and the effect of angle of attack is pronounced. At a lower angle of attack, the windward side has the wing and LEX vortices of considerable strength without merging or breakdown, and the leeward side has a concentrated LEX vortex and a weak wing vortex. At the higher angle of attack, a complete vortex breakdown occurred on the windward side, while the leeward wing and LEX vortices of considerable strength kept their identity.

Conclusion

The vortical flow of a delta wing with leading edge extension(LEX) was examined through off-surface visualization, 5-hole probe and hot-film measurements. The model was a flat wing with a 65° swept sharp leading edge. The angles of attack ranged from 10 to 30 degrees, and the sideslip angles ranged from 0 to -15 degrees. The Reynolds number was 1.82×10^5 for the flow visualization, and 1.76×10^6 for the 5-hole probe and hot-film measurements. The analysis is focused on the structure, interaction and breakdown of vortices depending on the angles of attack and sideslip.

The comparison of the visualization photos, the 5-hole probe and hot-film measurements showed that the results have an excellent agreement in relative positions and the structures of the wing and LEX vortices. The wing vortex and the LEX vortex coil each other while maintaining a comparable strength and identity at zero sideslip. By sideslip, the downward movement of the LEX vortex when going downstream was enhanced on the windward side, and the downward and inboard movement of the LEX vortex when going downstream, was suppressed on the leeward side. Also the counterclockwise coiling of the wing and LEX vortices was decreased on the leeward side. The increase of angle of attack shifted the core of the wing and LEX vortices inboard and upward, increased the coiling of the vortices and the diameter of spiraling. The sideslip amplified the vertical shift of the core position, especially on the leeward side.

Acknowledgement

This work was sponsored by the Korea Science and Engineering Foundation, under grant number R01-2000-000-00318-0.

References

1) Olsen, P. E., and Nelson, R. C., "Vortex Interaction over Double Delta Wings at High Angles of Attack," AIAA Paper 89-2191, July 1989.

2) Grismer, D. S. and Nelson, R. C., "Double-Delta-Wing Aerodynamics for Pitching Motions With and Without Sideslip," J. of Aircraft, Vol. 32, No. 6, 1995, pp. 1303-1311.

3) Hebbar, S. K., Platzer, M. F., and Chang, W., "Control of High-Incidence Vortical Flow on Double-Delta Wings Undergoing Sideslip", J. of Aircraft, Vol. 34, No. 4, 1997, pp. 506-513.

4) Sohn, M. H. and Lee, K. Y., "Experimental Investigation of Vortex Flow of a Yawed Delta Wing Having Leading Edge Extension", AIAA Paper 2002-3267, June 2002.

5) Hoeijmakers, H. W. M., Vaatstra, W., and Verhaagen, N. G., "Vortex Flow Over Delta and Double-Delta Wings", J. of Aircraft, Vol. 20, No. 9, 1983, pp. 825- 832.

6) Cunningham, A. M. and den Boer, R. G., "Low-Speed Unsteady Aerodynamics of a Pitching Straked Wing at High Incidence-Part II: Harmonic Analysis", J. of Aircraft, Vol. 27, No. 1, 1990, pp. 31-41.

7) Ericsson, L. E., "Vortex Characteristics of Pitching Double-Delta Wings", J. of Aircraft, Vol. 36, No. 2, 1999, pp. 349-356.

8) Erickson, G. E., Schreiner, J. A., and Rogers, L. W., "On the Structure, Interaction, and Breakdown Characteristics of Slender Wing Vortices at Subsonic, Transonic, and Supersonic Speeds," AIAA Paper 89-3345, August 1989.

9) Cunningham, A .M., Jr. and den Boer, R. G., "Steady and Unsteady Aerodynamics of a Pitching Straked Wing Model at High Angles of Attack", AGARD CP-494, Oct. 1990 (paper 29).

10) Sohn, M. H. and Lee, K. Y., "Effects of Sideslip on the High-Incidence Vortical Flow of a Delta Wing with the Leading Edge Extension", AIAA Paper 2003-1107, January 2003.